Pergamon

Cement and Concrete Research 29 (1999) 1713–1719

CEMENT AND CONCRETE RESEARCH

Hydration and strength development of binder based on high-calcium oil shale fly ash Part II. Influence of curing conditions on long-term stability

C. Freidin*

The Center for Desert Architecture and Urban Planning, The Jacob Blaustein Institute for Desert Research, Ben-Gurion University of the Negev, Sede-Boker Campus 84990, Israel

Received 15 September 1998; accepted 11 June 1999

Abstract

The distinguishing feature of high-calcium oil shale fly ash (HCOSFA) used in experiments is the high amount of free CaO and SO_3 in form of lime and anhydrite. Strength development as well as the microstructure and composition of the new formations of fly ash binder (FAB) based on HCOSFA and low-calcium coal fly ash after curing in different conditions and long-term exposure in various environments were studied. It was determined that moist air and water are the most favorable conditions for aging processes of FAB. In atmospheric air three stages in strength change of cured FAB are observed: increase of compressive strength over 1 month; sharp drop after 1 month up to the 3 to months; stabilization or slowdown of loss in strength after 3 to 6 months of exposure. The duration of the second and third stages depends on HCOSFA content and does not depend on curing conditions. One of the hydration products of FAB is ettringite. Its instability in air could be a reason for the decrease in strength of FAB and some disintegration of the hardened system. In the presence of low-calcium coal fly ash, additional amounts of stable calcium silicate hydrates are formed during FAB curing especially during steam curing. This has a positive effect on compressive strength and stability of FAB in atmospheric air.

Keywords: Compressive strength; Curing; Hydration products; Cement; Fly ash

1. Introduction

High-calcium fly ash such as oil shale fly ash from Jordan, Greek, Israel, and other countries that contain free CaO and SO_3 in form of lime and anhydrite possess pozzolanic activity as well as hydraulic properties. It can set and harden with water without any further additives [1–3]. Studies of high-calcium ashes formed by fluidized bed combustion process of Israel's oil shales showed that one of the products of the hydration is calcium aluminum trisulfate (AFt)-ettringite [4].

AFt is stable in an aqueous solution at temperatures up to 90°C and higher [5]. However, it reacts differently in air. Dehydration and carbonation processes, which can take place in air, reduce the amount of Aft; gypsum, calcium carbonate, and alumina gel are formed in its place [6,7]. In other words, the AFt-containing system can decompose and decrease its strength and consequently its stability.

These negative results of the AFt breakdown could be eliminated by formation of an additional amount of more stable binder phases in the initial stage of high-calcium fly ash curing. In Part I [8] it was shown that this effect can be obtained by a combined hydration of high-calcium fly ash and low-calcium fly ash. The interaction would give secondary high strength and more stable calcium silicate hydrates (CSH), which should improve the stability of the hardened system in atmospheric air.

The firmness of the systems containing high-calcium oil shale fly ash and low-calcium coal fly ash as well as the composition and microstructure of new formations after their curing in various conditions and after later long-term exposure to moist air, water, and atmospheric air are discussed in the present paper.

* Corresponding author. Tel.: +972-7-659-6876; fax: +972-7-659-6881.
E-mail address: freidin@bugmail.bgu.ac.il (C. Freidin)

0008-8846/99/$ – see front matter
PII: S0008-8846(99)00139-8

Table 1
Chemical composition and principal properties of fly ashes

	Chemical analysis (%) [ASTM 114]					Principal properties		
	HCOSFA	LCCFA				ASTM	HCOSFA	LCCFA
SiO_2	16.3	45.6	Density (kg/m^3)			C 188	2300	2500
Al_2O_3	5.6	33.5	Bulk specific gravity (kg/m^3)			C 29	690	810
Fe_2O_3	3.6	3.5	Fineness: passing the 45-μm (no. 325) sieve (%)			C 430	89.1	75.3
CaO_{total}	52.3	5.4	Water requirement (WR %)					
CaO_{free}	10.1	–				C 187	81.7	51.3
MgO	0.8	1.6	HCOSFA	LCCFA	WR	–	–	–
SO_3	10.7	0.4	80	20	75.5	–	–	–
P_2O_5	2.5	1.6	60	40	69.8	–	–	–
Na_2O	0.3	0.5	40	60	63.2	–	–	–
K_2O	0.4	0.3	20	80	57.7	–	–	–
Loss on ignition (950°C)	5.1	5.9	Soundness: autoclave expansion (%)			C 151	0.1	0.03

2. Experimental

2.1. Materials

High-calcium oil shale fly ash (HCOSFA) from the Pama plant, located in the Negev ("Developing Energy Resources LTD," Israel) was used in experiments (Table 1). HCOSFA is the waste product of burning local low-calorie oil shales. These oil shales contain 12–15% of organic matter in a matrix of calcite, quartz, fluorapatite [$Ca_{10}(PO_4)_6F_2$], and minor amounts of other crystalline and amorphous matter [9].

Oil shale is burned in the dust state in a fluidized bed combustor. The burning temperature ranges from 850 to 900°C. Fuel fine grains remain in fluidized bed combustion process for a few minutes on average and the crystalline phases in the resulting fly ash particles consists of anhydrite, calcite, lime, quartz, fluorapatite, and clinker minerals (β-C_2S, C_3A, and C_4AF) [3,4,8,10].

The generation of clinker minerals in HCOSFA may be explained as follows. Although the nominal combustion temperature is around 850–900°C, much hotter zones ("hot spots") with temperature well in excess of 1200°C exist. This produces the partial melting of the combustion ash and the local formation of the liquid phase in which clinker mineral-forming reactions are possible. The presence of calcite in fly ash is conditioned to the parameters of oil shale combustion (fluidized bed combustion). Low combustion temperature (850–900°C) and excess pressure do not allow for the complete calcination of calcite to lime and both calcite and lime are present in HCOSFA. Properties of HCOSFA are showed in Table 1.

Low-calcium coal fly ash (LCCFA) was obtained from the coal-burning power station in Hadera (Israel). Its chemical composition and the results of standard tests as defined by American Society for Testing and Materials are summarized in Table 1. It was found by X-ray diffraction (XRD) and scanning electron microscopy (SEM) analyses that the LCCFA consists of glassy spherical particles that incorporate mullite and quartz crystals [8].

High- and low-calcium fly ash binders (FAB) were prepared by mixing HCOSFA and LCCFA in a blade paddle mixer for 3–5 min. Standard tests indicated that the mixtures of HCOSFA and LCCFA (FAB) have a high water requirement (Table 1) compared to ordinary Portland cement (22–27%).

It is to be expected that such a high water requirement would give a low strength when testing FAB using normal consistency paste specimens. Similar results were obtained by others, who determined the strength of HCOSFA based binder in cast paste specimens with a large proportion of mixing water [4,5]. However, their experiments, performed with compacted HCOSFA mortar specimens, showed that the strength values of binders obtained are high enough to recommend their application as a cementing material for production of compacted (pressed) building units such as blocks, bricks, and tiles [11]. Current research takes this recommendation into account. The stability tests of HCOSFA and LCCFA binders were done using pressed specimens to simulate their possible utilization as a cement substitute for pressed building products.

Natural quartz sand used as a part of the mortar specimens has a density of 2610 kg/m^3, a bulk specific gravity of 1470 kg/m^3, and the fineness modulus of 2.83.

2.2. Experimental procedure

Pressed mortar specimens (cylinders of 5.70 cm in height and diameter) were used in order to determine the effect of

Table 2
Mortar compositions (%, by weight)

Mortar	Dry components			Mixing water (from dry components)
	HCOSFA	LCCFA	Sand	
1	12	48	40	25
2	24	36	40	25
3	36	24	40	25
4	48	12	40	25
5	60	–	40	30

Table 3
Curing and exposure conditions

Initial curing conditions	Exposure conditions	Mortar (#)	Fig.
Moist air			
1 day	Water exposure	Mortar 3	1
1 day	Moist air exposure	Mortar 3	1
3 days	Atmospheric air exposure	Mortar 1	2
3 days	Atmospheric air exposure	Mortar 2	2
3 days	Atmospheric air exposure	Mortar 3	2
3 days	Atmospheric air exposure	Mortar 4	2
3 days	Atmospheric air exposure	Mortar 5	2
3 days	Atmospheric air exposure	Mortar 2	3
Steam curing			
60° C	Atmospheric air exposure	Mortar 2	3
90° C	Atmospheric air exposure	Mortar 2	3

curing conditions (moist and steam curing) and exposure conditions (moist air, water, and atmospheric air) on the compressive strength of FAB. Five different compositions of mortar were used (Table 2).

Raw mixtures for mortar specimens were prepared by adding sand and water to preprepared FAB and blending them until the mass was homogeneous. Pressed paste specimen disks of 15 mm in height and 57 mm in diameter were designed for investigating the composition and microstructure of FAB after moist curing and steam curing, as well as after long-term exposure of cured FAB in atmospheric air. The FAB consisted of 60% HCOSFA and 40% LCCFA. Specimens were compacted from a mixture with mixing water (MW) at 30%.

All test specimens were molded on a Carver laboratory hand press at a compaction pressure of 4 MPa. Test specimens cured and were exposed to various conditions:

- moist air at constant temperature (20 ± 3°C) and humidity (RH > 96%)—moist curing and moist-air exposure;
- water at a temperature between 20–23°C—water curing and water exposure;
- atmospheric air at a temperature between 18–23°C and RH of 35–60%—atmospheric air exposure;
- steam atmosphere (temperatures of 60 and 90°C, duration of 8 h) steam curing.

In Table 3 various curing and exposure conditions of the above-mentioned specimens can be seen. After curing and exposure, the mortar specimens were crush-tested to determine compressive strength through the certain period. The paste specimens were examined by XRD analysis and SEM to find a composition and structure for new formations of the cementing matter of FAB.

3. Results and discussion

3.1. Influence of curing and exposure conditions on compressive strength of fly ash binders

3.1.1. Moist air and water

The typical curves showing change of Mortar 3 specimens' compressive strength in moist air and in water for 36 months are alike (Fig. 1). A continuous curing and increasing compressive strength of FAB were observed throughout the experiment (Fig. 1). These processes progressed rapidly in the initial period (up to 3 months) and strength reached 60–65% of 36-month values. Thereafter, strength growth was slowed. After 18 months strength stabilization was evident. It should be noted that curing in water was more effective than in moist air; compressive strength in water was greater than in moist air.

3.1.2. Atmospheric air

In Fig. 2 test results showing the influence of HCOSFA content on compressive strength of cured FAB in atmospheric air are presented. Several conclusions can be drawn. There are three clearly distinguishable stages in strength development curves:

In the first stage, which generally takes one month, an increase in strength can be observed. This is caused by loss of water, drying, and a gain in compressive strength of the specimens.

The second stage (from the second to the sixth month) is marked by a sharp drop in strength. The severity of

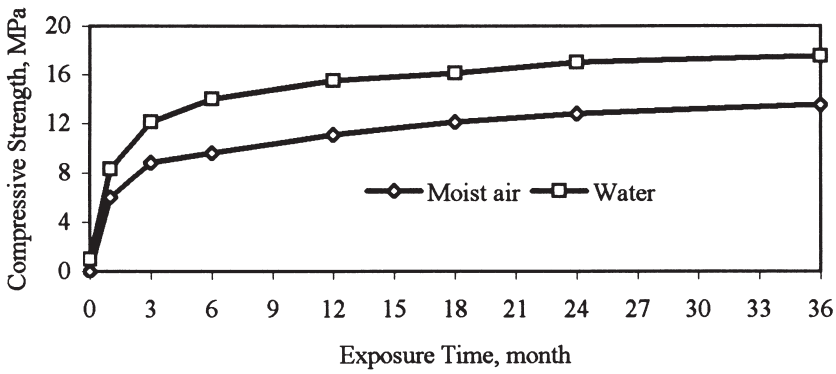

Fig. 1. Compressive strength of cured FAB in moist air and water; mortar 3 (Table 2).

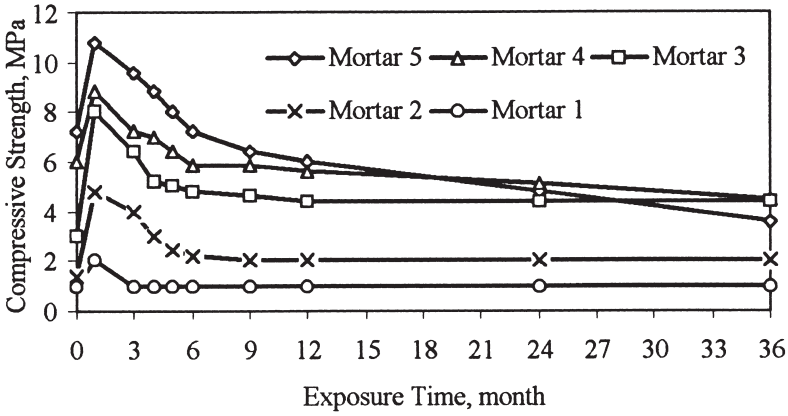

Fig. 2. Effect of HCOSFA content on development of FAB compressive strength in atmospheric air; mortars 1–5 (Table 2).

loss depends on the initial strength (compressive strength of specimens after 3 days of previous moist curing) that in turn is determined by the HCOSFA content. Specimens with low initial strength (12 and 24% HCOSFA) reached the end of the decrease in compressive strength sooner (during 2 to 4 months), while specimens with higher initial strength (36 and 48% HCOSFA) lost their compressive strength more sharply and over a longer period of time (4–6 months). Evidently this deterioration is caused by destructive processes within AFt. Their duration depends on the initial quantity of AFt in cured specimens.

The third stage of strength development curves is characterized by stabilization of strength at its initial level (24 and 36% HCOSFA) or at an even higher level (12% HCOSFA). Specimens with a higher HCOSFA content (48%) do not come to full stabilization, but the loss of compressive strength only slows down, similar to specimens without LCCFA that serve as reference in this study. Such a change in strength suggests that the decay of AFt is not yet completed by the end of this experiment and may continue in the future—further studies will be needed.

Fig. 3 shows an effect of curing conditions on FAB strength change in atmospheric air. It can be seen that curves of strength development have three stages independent of curing conditions. The first stage displays an increase in strength for the first month of specimens exposure to atmospheric air. The second stage reflects a loss of strength, which happens because of destructive processes that occur in cured FAB for the later 2 to 5 months. The strength of specimens cured under steam treatment was reduced significantly less than that of moist-cured specimens; the greater the temperature, the smaller the loss. The third stage, starting at 3–6 months, shows that strength-degrading changes in cured FAB are reduced. Between 6 to 12 months, the changes appear to stop and the compressive strength of specimens remains at a constant value. The fastest strength stabilization (6 months of air exposure) comes for specimens cured in a steam atmosphere at 90°C.

3.2. Composition and structure of fly ash binder after curing and exposure in various conditions

3.2.1. XRD analysis

XRD patterns of FAB paste specimens (60% HCOSFA + 40% LCCFA; W/B = 30%) after moist and steam curing

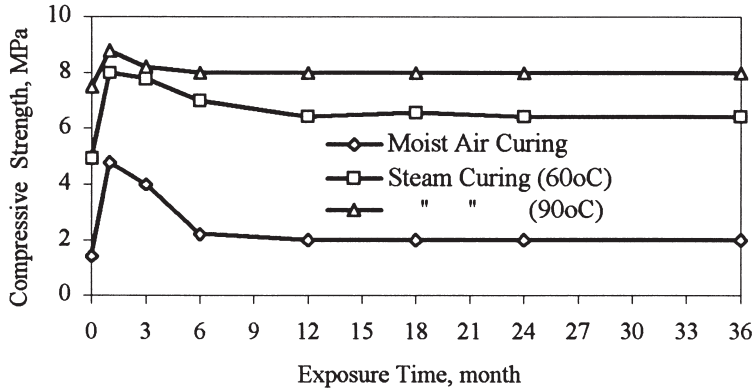

Fig. 3. Effect of curing conditions on development of FAB compressive strength in atmospheric air; mortar 2 (Table 2).

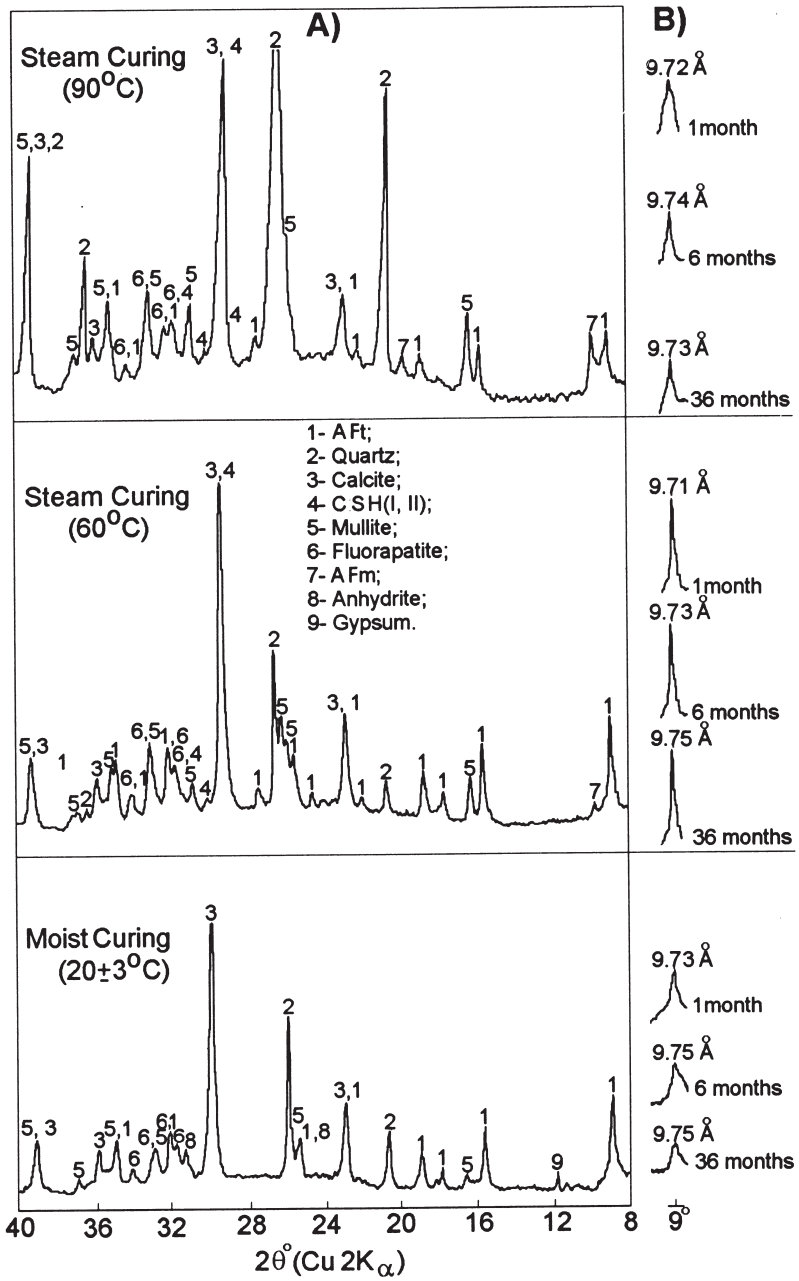

Fig. 4. XRD patterns: (A) full patterns of cured FAB; (B) AFt peak segments in patterns of cured FAB after atmospheric air exposure.

(A) as well as the AFt segment of patterns after long-term exposure of cured FAB in atmospheric air (B) are presented in Fig. 4. The presence of AFt (1), quartz (2), calcite (3), mullite (5), and fluorapatite (6) peaks are common to all XRD patterns (Fig. 4A). Differences are in the following points:

1. Intensity of XRD pattern peaks (1) for the steam-cured binder is higher than for the moist-cured binder. This could be explained by a greater extent of crystallization of hydration products in curing processes carried out at higher temperature.
2. The XRD pattern of moist-cured binder has peaks of anhydrite (8) and gypsum (9). The same peaks are absent in XRD patterns of steam-cured FAB.
3. The XRD pattern of moist-cured FAB has no peaks of CSH. This may be linked to X-ray amorphousness of CSH. However, there is circumstantial evidence of their presence as described elsewhere [8]: “The analysis of HCOSFA content effect on strength of FAB shows that in spite of decrease of HCOSFA amount in specimens from 60% to 48–36%, i.e. on 20–40%, by substitution with LCCFA their compressive strength was close to that of specimens contained only

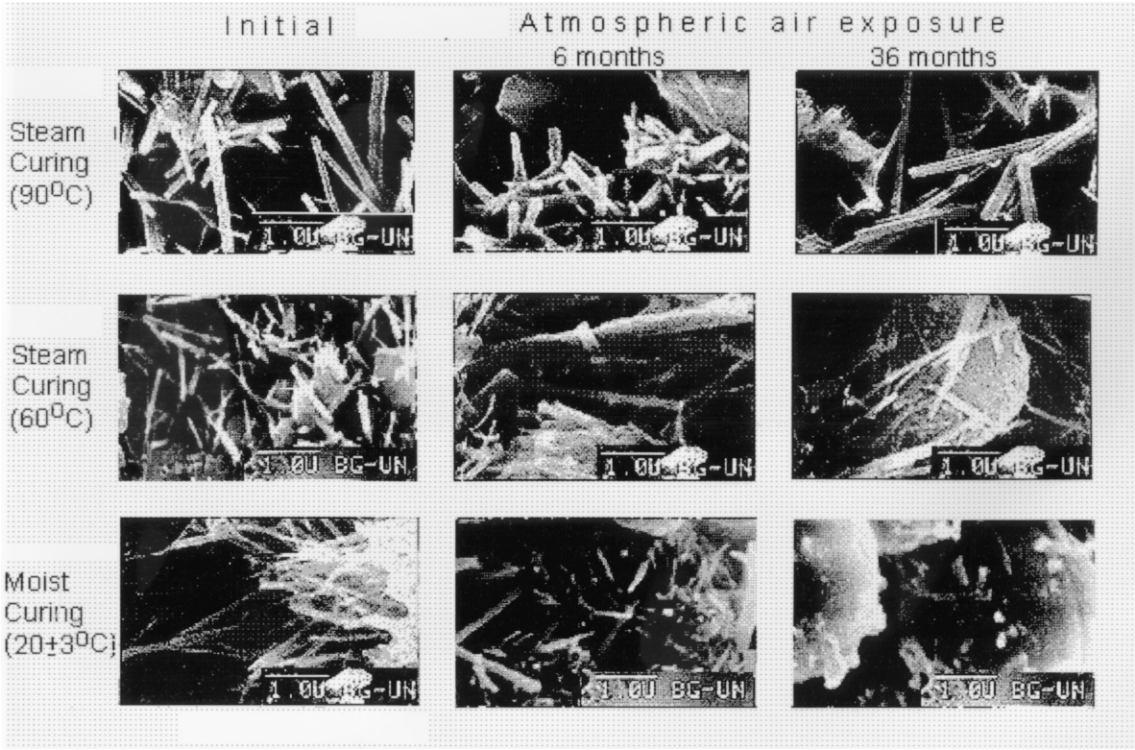

Fig. 5. Scanning electronic microscopy observations of ettringite phases in cured FAB (15,000× magnification).

HCOSFA (90–95%). This can be attributed only to an interaction of CaO_{free} of HCOSFA and active SiO_2 of LCCFA with producing the additional cementing matter in form of CSH." The possibility of such a mechanism of formation for CSH is also confirmed by the absence of lime and CH peaks in the XRD pattern of moist curing FAB (Fig. 4A). The lime peak was defined in XRD pattern of raw HCOSFA [10]. The increase of curing temperature is favorable to forming CSH phases and their crystallization. Finally, XRD patterns of steam-cured FAB at 60 and 90°C have peaks with $d = 2.81$ and 2.97 Å (Fig. 4), which can be attributed to calcium silicate hydrate ($CaO \cdot SiO_2 \cdot H_2O$) in the form of CSH(I, II). The CSH strengthens hardened binder and can improve its stability in different conditions.

4. In addition to AFt peaks (1), XRD patterns of steam-cured FAB have peaks with $d = 8.86$ and 8.93 Å (Fig. 4) were attributed to calcium monosulfate hydrate (AFm): $3CaO \cdot Al_2O_3 \cdot CaSO_4 \cdot 12H_2O$. In all likelihood its formation is connected to the important role that the reaction of CaO_{free} of HCOSFA and active SiO_2 of LCCFA plays in the FAB curing process. It decreases the concentration of CaO_{free} in the liquid phase of the cured system. A prerequisite in generating more stable low-basic calcium hydrate aluminates is created. The development of this reaction predetermines the formation of AFt only in the initial stage of FAB curing. Later the trisulfate form partially converts to AFm; the greater the temperature of curing, the greater the quantity that is formed. Thus, the intensity of the AFm peak (7) in the XRD pattern of steam-cured FAB at 90°C is higher than that at 60°C.

The XRD pattern segments of open air-exposed specimens of cured FAB, which belong to AFt only (Fig. 4B), indicate a marked reduction in the intensity of the 9.73–9.75 Å ettringite peaks for moist-cured specimens. This is due to a decomposition of AFt. At the same time, AFt peak intensity in XRD pattern segments of steam-cured specimens is hardly changed.

3.2.2. Microstructure observation

The ettringite phase is of the highest interest compared to other hydrate products of FAB since its stability under various conditions influences binder durability. In Fig. 5 the morphologic features of AFt both after curing of the FAB and after 6- and 36-month exposure of cured FAB to atmospheric air can be seen.

Comparison of the initial images after FAB curing shows that AFt produced at higher temperatures (60 and 90°C) is much more crystallized and has less specific surface area than that formed during moist curing at 20 ± 3°C. These microstructures are consistent with the observation that atmospheric air exposure caused less of a reduction in the strength of steam-cured FAB than of moist-cured FAB (Fig. 3). AFt microstructure of steam-cured FAB showed less alteration with time than that observed for the moist-cured FAB (Fig. 5).

4. Conclusions

The following conclusions concerning the durability of fly ash binder based on high-calcium oil shale and low-calcium coal fly ash can be made.

1. The durability of binder may be evaluated by monitoring long-term strength in various conditions.
2. The continuous increases of FAB compressive strength are observed under moist air and water conditions.
3. In atmospheric air there are three stages in strength change of cured FAB: increase of compressive strength for 1 month, sharp drop after 1 month up to the 3 to 6 months, and stabilization or gradual loss in strength after 3 to 6 months of exposure.
4. The duration of the second and third stages depends on HCOSFA content and does not depend on curing conditions.
5. Combined hydration of high-calcium oil shale fly ash and low-calcium coal fly ash gave an additional amount of high strength and stable CSH, which neutralizes the effect of decay in the ettringite and improves the durability of the hardened system in atmospheric air. However, a decrease in strength during a certain period of exposure to atmospheric air (2–5 months) was still noted.

Acknowledgments

The author would like to express his appreciation for the research grant from the Jacob Blaustein Institute for Desert Research, Ben-Gurion University of the Negev (Israel) to carry out the reported work, which forms part of the major research program on the development of technology of cementless building materials on the basis of fly ashes.

References

[1] T. Khedaywi, A. Yeginobali, M. Smadi, J. Cabrera, Pozzolanic activity of Jordan oil shale ash, Cem Concr Res 20 (1990) 843–852.
[2] V.G. Papadakis, E.J. Pedersen, Effects of high-calcium fly ash, low-calcium fly ash and silica fume on mortar properties, Proc. 6th Int. Conf. on Fly Ash, Silica Fume, Slag and Natural Pozzolans in Concrete, Supplementary Papers, 1998, pp. 355–370.
[3] A. Bentur, M. Ish-Shalom, M. Ben-Bassat, T. Grinberg, Properties and application of oil shale ash, Proc. 2d Int. Conf. on Fly Ash, Silica Fume, Slag and Natural Pozzolans in Concrete, 1986, pp. 779–802.
[4] A. Bentur, M. Ish-Shalom, M. Ben-Bassat, T. Grinberg, Cementing properties of oil shale ash: Part I, II, and III, Cem Concr Res 10 (1980) 175–182; 11 (1981) 645–650; 11 (1981) 799–807.
[5] V. Satava, O. Veprek, Thermal decomposition of ettringite under hydrothermal conditions, J Am Ceram Soc 58 (7–8) (1975) 357–358.
[6] R.K. Mehta, Stability of ettringite on heating, J Am Ceram Soc 55 (11) (1972) 55–56.
[7] T. Nashikawa, K. Suzuki, T. Takabe, Decomposition of synthesized ettringite by carbonation, Cem Conc Res 22 (1992) 6–14.
[8] C. Freidin, Hydration and strength development of binder based on high-calcium oil shale fly ash, Cem Conc Res 28 (1998) 829–839.
[9] L. Heller-Kallai, G. Esterson, Z. Aizenshtat, M. Pismen, Mineral reactions and pyrolysis of Israeli oil shale, J Anal Appl Pyrolis 6 (1984) 375–389.
[10] O. Yoffe, Y. Nathan, The chemistry and mineralogy of ashes from PAMA demonstration plant, Proc. 12th Israeli Conference the Israel Assoc for the Advancement of Mineral Engineering, 1994, pp. 270–274.
[11] A. Bentur, Application of oil shale ash as building material, Silicates Industrials, Silic Industr 7/8 (1982) 163–168.